Extended hybridization and energy transfer in periodic multimaterial organic structures in strong coupling with surface plasmon

Antoine Bard, Sylvain Minot, Clémentine Symonds, Jean-Michel M Benoit, Alban Gassenq, François Bessueille, Bruno Andrioletti, Camilo Perez, Kévin Chevrier, Yannick De Wilde, et al.

Extended hybridization and energy transfer in periodic multimaterial organic structures in strong coupling with surface plasmon

*Antoine Bard, Sylvain Minot, Clémentine Symonds, Jean-Michel Benoit, Alban Gassenq, François Bessueille, Bruno Andrioletti, Camilo Perez, Kévin Chevrier, Yannick De Wilde, Valentina Krachmalnicoff, and Joel Bellessa**

A. Bard, S. Minot, C. Symonds, J.M. Benoit, A. Gassenq, J. Bellessa
Univ Lyon, Université Claude Bernard Lyon 1, CNRS, Institut Lumière Matière, F-69622, Villeurbanne, France
E-mail: joel.bellessa@univ-lyon1.fr

S.Minot, F. Bessueille
Université de Lyon, CNRS, Université Claude Bernard Lyon 1, Institut des Sciences Analytiques, UMR 5280, 5 rue de la Doua, F-69100 Villeurbanne, France.

B. Andrioletti
Université de Lyon, Université Claude Bernard Lyon 1, ICBMS UMR CNRS 5246, 1, Rue Victor Grignard, 69622 Villeurbanne cedex, France.

C. Perez, K. Chevrier, Y. De Wilde, V. Krachmalnicoff
Institut Langevin, ESPCI Paris, Université PSL, CNRS, 75005 Paris, France

Keywords:
Plasmon
Strong light matter coupling
Energy transfer
Metasurfaces

Abstract:

The strong light matter coupling occurring when the light matter interaction prevails on the damping, has found applications beyond the domain of optics, in chemistry or transport. These advances make crucial the development of various structures in strong

coupling. In this paper we propose a new way to hybridize two materials and transfer energy through a surface plasmon over micrometric distances. For this purpose, two patterned interlocked dyes arrays, one donor and one acceptor, are deposited on a silver surface by successive micro contact printing, leading to a pattern of 5 microns period. The dispersion relation of the structure is measured with reflectometry experiments and evidence the hybridization with the plasmon, and the formation of states mixing both excitons and the plasmon with similar weights. The mixing in these polaritonic metasurfaces enables an energy transfer mechanism in strong coupling, which is observed with luminescence experiments. As the donor and acceptor are spatially separated by a distance larger than the diffraction limit the excitation transfer is directly measured, and evaluated by comparison with dyes arrays without silver.

1. Introduction

The coupling of different molecules over large distances mediated by the strong interaction with a photonic or a plasmonic mode finds applications in the field of optics, but also well beyond, in electrical transport,[1] chemistry,[2] or magnetism.[3] In this strong coupling regime, the light and the molecular excited states cannot be considered separately and are hybridized to form polaritons.[4,5] One of the key feature of this hybridization lies in the coupling of otherwise independent oscillators. The basic idea is that the hybridized state between an extended optical state and localized molecules results in a coupled coherent state involving a large number of molecules, spread over the optical/plasmonic mode extension. [6,7] Different demonstrations have been achieved [8,9] showing the coherence and extension of the hybridized state. The generation of extended coherent states can modify the transport properties of the molecules: a demonstration of conductivity enhancement has been performed. [1,10,11] The molecular extension mediated by strong coupling could also play a key role in chemistry. [12-14] The energy structure of molecular materials can be tailored by patterning the organic material within the coherence length. The obtained structure presents properties that average the different patterns constituting the surface but are sensitive to the geometry of the pattern. These behaviours are characteristic of metasurfaces [15] but polaritonic metasurfaces differ from usual metasurfaces because of the polariton extension which can exceed the wavelength by one or several orders of magnitude. [16]

The inclusion of different materials in a system in strong coupling in adequate conditions leads to the formation of hybrid states that mix the excitons of each material. Several demonstrations

of the hybridization of molecular states have been performed. [17-20] A particular application of this hybridization is the enhanced energy transfer between both materials, one donor and one acceptor, when they are in strong coupling. The energy is transferred through an intermediate state comprising contributions of donor and acceptor (middle energy polariton). [21,22] As long as both donor and acceptor are hybridized together through the optical mode the energy transfer remains efficient. [23] This non-radiative energy transfer in strong coupling, like Forster energy transfer, modifies the donor emission rate. It has been demonstrated with time resolved experiments for separation up to 100 nm, [23] to be compared with distances smaller than 10 nm for the Förster process. Very recently a demonstration of energy transfer in an extended microcavity in strong coupling has shown luminescence transfer up to 2 μm. [24] All these demonstrations have been performed on stacked layers in microcavities. The extension of polaritonic states could be advantageously applied to couple different materials laterally separated on a surface, providing flexibility to the material arrangement and easy access to the materials. The complete lateral separation of two materials in strong coupling over micrometric distances could also be useful for sources using polaritons, as polariton lasers. [25,26] Indeed, the distance obtained are compatible with separated emission and excitation, whether optical or electrical: the coherence length is larger than the diffraction limit in the visible range and also larger than diodes typical sizes.

In this paper we exploit the extension of hybrid states to mix two different molecular materials through a surface plasmon. We develop a multimaterial system based on two structured dye layers, fully spatially separated, arranged in a square lattice with a 5 μm period and deposited on a silver film. We evidence a new type of multimaterial metasurface based on the hybridization of both materials excited levels with the plasmon, and the formation of hybrid states mixing the organic materials and the plasmon. Beside the control of the energy states allowed by the geometry and averaging, these structures also show transfer of emission from one dye to the other.

2. Fabrication of bi-material arrays

To investigate the effect of spatial separation on the hybridization, we design two structured dye layers, one formed by a periodic array of disks, and the other by the complementary structure, namely a film perforated by holes. Both are deposited on a silver layer. To evidence the effect of the spatial separation, samples with the two dye superposed and with the dyes separated have been fabricated. A layout of the sample is shown in **Figure 1a** and **1b**.

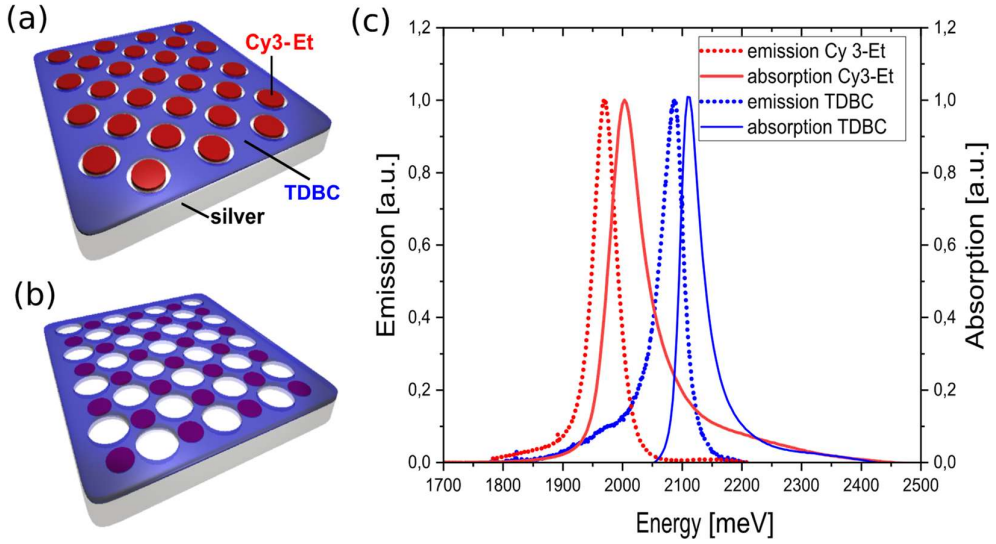

Figure 1. Sketch of the sample in the areas where a) Cy3-Et disks are inserted in the holes of the TDBC layer, b) Cy3-Et disks are located under the TDBC layer. c) Normalized absorptions (solid lines) and emission (dashed lines) of TDBC (blue) and Cy3-Et (red) films.

As organic materials, we chose two J-aggregated cyanine dyes whose absorptions are spectrally distinct: 5,6-Dichloro-2-[[5,6-dichloro-1-ethyl-3-(4-sulfobutyl)-benzimidazol-2-ylidene]-propenyl]-1-ethyl-3-(4-sulfobutyl)-benzimidazolium hydroxide, inner salt, sodium salt (TDBC), and 5-Chloro-2-[2-[5-chloro-3-(4-sulfobutyl)-3H-benzothiazol-2-ylidenemethyl]-but-1-enyl]-3-(4-sulfobutyl)-benzothiazol-3-ium hydroxide, inner salt, triethylammonium salt (Cy3-Et) from Few Chemicals. The dyes can be diluted in aqueous solution, a solvent suitable for a self-association of the monomers to form a J-aggregate structure. [27] J-aggregated dyes are used in this study because they present a narrow absorption linewidth associated to a high oscillator strength, and thus are very efficient to reach the strong coupling regime. [28] The absorption and emission spectra of TDBC and Cy3-Et are presented in **Figure 1c**. The TDBC absorption peak lies at 2109 meV, and has a full width at half maximum (FWHM) of 47 meV, while the Cy3-Et absorption is at 2000 meV with a FWHM of 73 meV. The energy separation between the absorption of both dyes is thus 109 meV, larger than their linewidths. Moreover, TDBC and Cy3-Et both present a strong emission band, located at 2086 and 1938 meV, respectively.

In order to spatially separate the two emitters, we have superimposed on a silver film two types of layers: one array of Cy3-Et disks, and one TDBC thin film perforated by circular holes. To obtain these two patterns, polyelectrolytes multilayers (PEMs) of each dye were fabricated by Layer-by-Layer assembly on microstructured PDMS stamps. [29] These stamps were fabricated by replica molding against silicon masters obtained via standard lithography and reactive ion etching (RIE) processes. The LBL method consists in alternatively dip the stamp in electrolytes of different polarity, one of these being the dye solution and the other a cationic solution of poly(diallyldimethylammonium chloride) (PDAC). [30,31] This approach is well suited for the deposition on non-planar substrates like the PDMS stamps. For the Cy3-Et layer an assembly of 8 Cy3-ET/PDAC bi-layers was formed on a stamp patterned in a square array of 4 µm diameter disks, with a p = 5 µm period. The negative stamp is used to obtain the perforated TDBC film formed by 12 TDBC/PDAC bi-layers. The disks size and array period were chosen to ensure a 50 % dye filling factor for each layer. The sample was obtained by first transferring the Cy3-Et PEMs microdisks by micro-contact printing (µCp) on a 50 nm silver film sputtered on a glass substrate. The PEMs of perforated TDBC was then printed on top of this stack. The fabrication method is summarized in **Figure 2**. To exactly locate the Cy3-Et disks in the holes of the perforated TDBC layer, the second stamp is slightly rotated compared to the first one, to introduce a small angle between the two arrays of patterns. Due to the Moiré effect, this leads to the formation of two types of regions on the sample. In the first kind of region, the Cy3-Et disks are located inside the holes of the TDBC thin films, and both emitters are in contact with the silver layer (Figure 1a). The diameter of the Cy3-Et disks has been chosen slightly smaller than the holes' diameter, as can be seen in an AFM image of this area (last panel of Figure 2), hence both emitters are spatially laterally separated. The angle between the stamps is small enough to ensure large regions of spatially separated dyes. Outside these regions the Cy3-Et disks are located under the TDBC film, leading to a stack of Cy3-Et/TDBC PEMs on silver (Figure 1b).

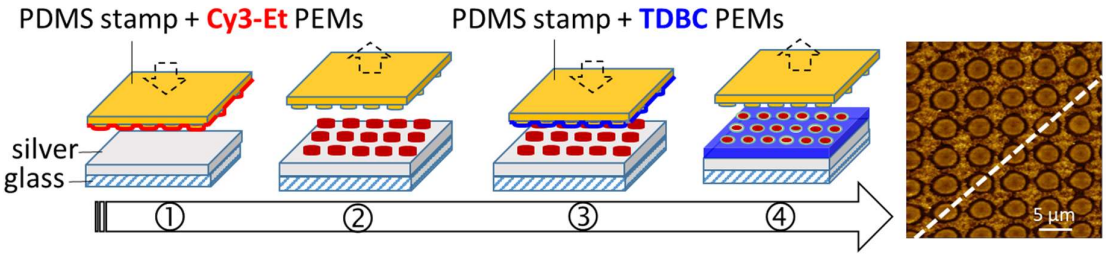

Figure 2. Sketch of the sample fabrication. An AFM image of an area where the Cy3-Et disks are inserted in the holes of the TDBC film is presented in the last panel. The dashed line in this image corresponds to the detected direction in the optical setup.

3. Long range hybridization through plasmon strong coupling

A leakage radiation microscopy setup was used to investigate the dispersion and energy levels of the system. The sample is placed on a large numerical aperture (N.A.) immersion objective (N.A. = 1.49), with the glass side in contact with the immersion oil to ensure refractive index continuity. The Fourier plane of the objective is imaged on the entrance slit of a spectrometer, selecting a given direction of the propagation wavevector. After spectral dispersion, the image recorded on a CCD camera can be associated to a dispersion relation: the vertical axis is related to the angle, and the horizontal axis to the wavelength. After a numerical treatment the dispersion relation E(k) of the modes can then be obtained, either in reflectometry by using a white light source in backscattering configuration or in luminescence by exciting the top side of the sample by a 532 nm laser. All the dispersion relations were recorded in TM configuration, with a detected wavevector direction oriented at 45° compared to the main axis of the square lattice, as shown by the dashed line in the AFM image of Figure 2.

In a first step, reflectometry experiments were performed on the area of the sample where the dyes are laterally separated, i.e. where the Cy3-Et disks are located in the holes of the TDBC film (Figure 1a). The resulting dispersion relation is shown in **Figure 3a**. Three main dispersive lines can be seen on this image (identified with black crosses). The upper and lower energy lines clearly show a curvature at the bare excitons energies characteristic of the strong coupling regime: instead of crossing, the bare plasmon and the excitonic transitions (horizontal dashed lines on the dispersion image) show an anticrossing. The clear anticrossing around 2100 meV indicates that both dyes cannot be treated independently. Indeed, in such a case the anticrossing with TDBC would be superposed to a plasmonic line lightly coupled to Cy3-Et, and would cross the bare excitonic line at 2100 meV.

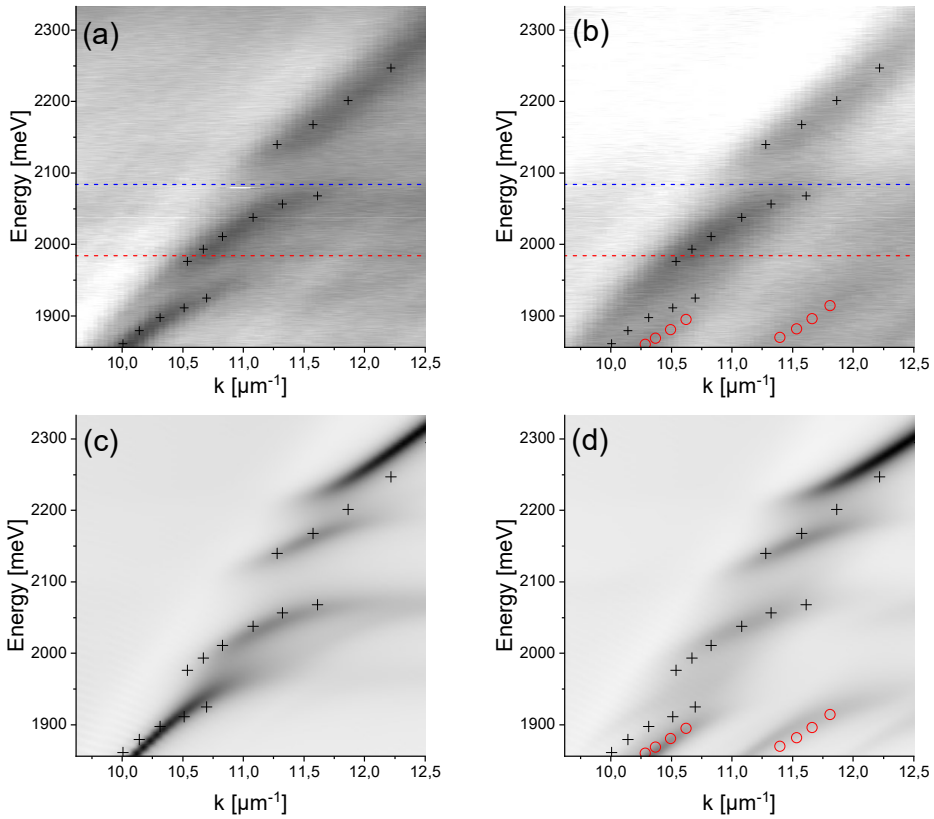

Figure 3. Experimental (top) and FDTD (bottom) dispersion images obtained in the areas where: a) and c) both dyes are laterally separated; b) and d) both dyes are superposed. The horizontal blue and red dashed lines indicate the energy positions of the uncoupled TDBC and Cy3-Et excitons, respectively. The black crosses indicate the positions of the three polaritonic dispersion lines identified in panel a) and are reported in the others images. The open red circles mark the low energy polariton and diffracted order of panel b) and are reported on panel d).

Reflectometry experiments were also carried out on the area where the Cy3-Et disks are printed outside the holes, i.e. located under the TDBC film (Figure 1b). The corresponding dispersion image is shown in **Figure 3b**. For the sake of comparison with the data obtained when the dyes do not overlap, the black crosses associated with the polaritonic lines of Figure 3a are reported on this graph. Very interestingly, there is a very good superposition of the two datasets for the upper and middle polariton branches. The lower branch, marked by red open circles, show a slight shift with respect to the polaritonic line observed for non-overlapping dyes. The first diffracted order of the low energy polariton line is also observable on the bottom right part of the image. The diffracted line is shifted by ~ 1 μm^{-1} from the low energy polariton line, in good agreement with the periodicity of the structure in this direction of propagation ($\frac{2\pi}{p\sqrt{2}} = 0.88$ μm^{-}

[1]). The similarity between the dispersions of Figure 3a and 3b is a strong indication of the key role played by the extension of the polaritonic state: whether the dyes are separated or stacked on the silver layer, the energy shifts from the bare states are mainly related to the number of molecules within the mode extension.

To compare our experimental results and confirm the main trends, the dispersion relations for both sample configurations were calculated with a 3D FDTD simulation, and presented in **Figure 3c** and **3d**. The simulations have been performed using the software Lumerical. Disks of Cy3-Et with a diameter of 3.75 µm and a TDBC layer with holes of 4.25 µm diameter were organised in an array of 5 µm period. The thickness used for both dyes is 13 nm and their energy and linewidth are extracted from Figure 1c. A good agreement between the calculation and the experiments is obtained for both structures. A splitting around 2200 meV obtained on the FDTD dispersion is not observed on the experimental data, probably because of experimental broadening. The order of magnitude of the polaritonic propagation length in amplitude can be evaluated for the middle polariton branch as 4 µm from the dispersion of **Figure 3a** (Δk=0.5µm^{-1} at k=11µm^{-1}) and 5µm from the FDTD calculations (Δk= 0.4µm^{-1}).

To go deeper in the interpretation and the understanding of the strong coupling in this spatially separated system, the energy levels extracted from the dispersion have been compared to a three level model. The main interest of this calculation in our context is the determination of the coupling energies between plasmon and excitons and the weight of the different exciton in the hybrid states. The dispersion relations can be obtained by diagonalizing the following Hamiltonian:

$$\begin{pmatrix} E_{pl}(k) - i\gamma_{pl} & V_{TDBC}/2 & V_{Cy3-E}\ /2 \\ V_{TDBC}/2 & E_{TDBC} - i\gamma_{TDBC} & 0 \\ V_{Cy3-E}\ /2 & 0 & E_{Cy3-Et} - i\gamma_{Cy3-E} \end{pmatrix}$$

where $E_{pl}(k)$ is the uncoupled surface plasmon energy as a function of the wavevector, γ_{pl} the plasmon homogeneous broadening, E_{TDBC} and $E_{Cy3\text{-}Et}$ the bare excitons energies, γ_{TDBC} and $\gamma_{Cy3\text{-}Et}$ their respective transitions linewidths. The interaction energies between each exciton and the plasmon resonance are noted V_{TDBC} and $V_{Cy3\text{-}Et}$. The dispersion relation of the bare plasmon mode was deduced by fitting the experimental reflectivity on an energy range far from the excitonic resonances (between 750 nm and 800 nm). For this purpose, we modelled the sample by a silver film covered by a continuous dielectric layer of refractive index n=1.75 with transfer

matrix method. The total thickness of the equivalent dielectric layer used for this fitting is 11 nm. The polaritonic dispersions obtained when using coupling strengths of V_{TDBC} = 90 meV and $V_{Cy3\text{-}Et}$ = 90 meV are presented in solid lines in **Figure 4a**, and are in very good agreement with the experimental reflectometry data (black crosses). The green dashed line corresponds to the bare plasmon mode, the dashed horizontal lines at 2084 meV and 1984 meV to the bare excitonic states used in the calculation. The energy splitting between the three branches is thus larger than the respective linewidth of the bare states, and of the same order of magnitude than the energy separation between the two excitonic states. To go further, we calculated the plasmonic and excitonic weights of each polaritonic branches. The high (resp. low) energy polaritonic line presents an almost 50% mixing of plasmon and TDBC (resp. Cy3-Et) exciton at the resonance. Around 11 μm^{-1}, the middle polaritonic branch is formed by a mixing of both excitons (30% each) and plasmon (40%) (**Figure 4b**). This proves that this system leads to the formation of an extended hybrid state where both emitters, although spatially separated, are mixed together through their strong coupling with the plasmon mode. We demonstrate here that the metasurface effect already shown for a single dye structured on metal for period smaller than the coherence length[16] can be extended to multimaterial systems.

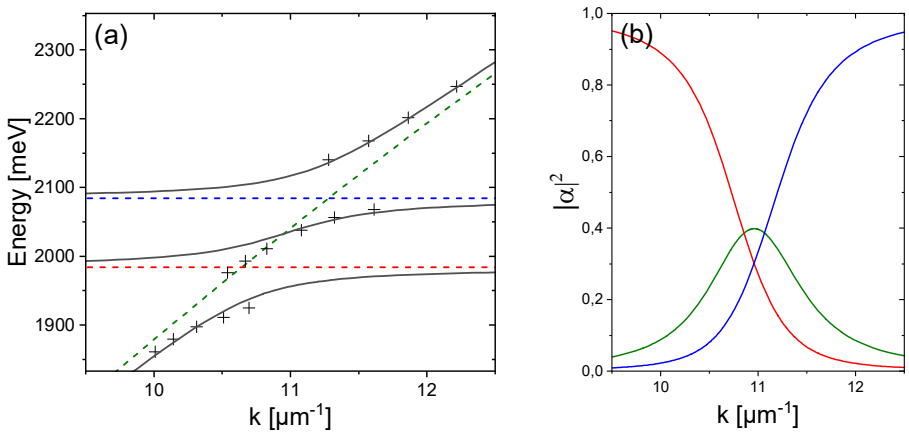

Figure 4. a) Polariton dispersion relations obtained by the three level coupled oscillators model. The dashed lines correspond to the energies of the uncoupled surface plasmon (green), TDBC (blue) and Cy3-Et (red) excitons. The black crosses correspond to the positions of the experimental dispersion lines of Figure 3a. b) Middle energy branch Hopfield coefficients associated to plasmon (green), TDBC (blue) and Cy3-Et (red) excitons.

4. Energy transfer in bi-materials metasurfaces

In order to investigate the energy transfer between the two excitonic transitions now coupled together, we study the luminescence on a region with spatially separated dyes (Cy3-Et disks located in the holes of the TDBC film). In a first step, we performed experiments with a spatially localized excitation at 532 nm. As the period of the polaritonic metasurface is larger than the diffraction limit [16], it is possible to excite selectively the TDBC dye, which can be seen as the donor for energy transfer. To evidence the contribution of polaritons, we compare the separated dye pattern deposited on silver with a reference sample where the same pattern is deposited directly on glass. The **Figure 5a** is a spatial luminescence image of the sample with an excitation laser spot extended over the whole structure.

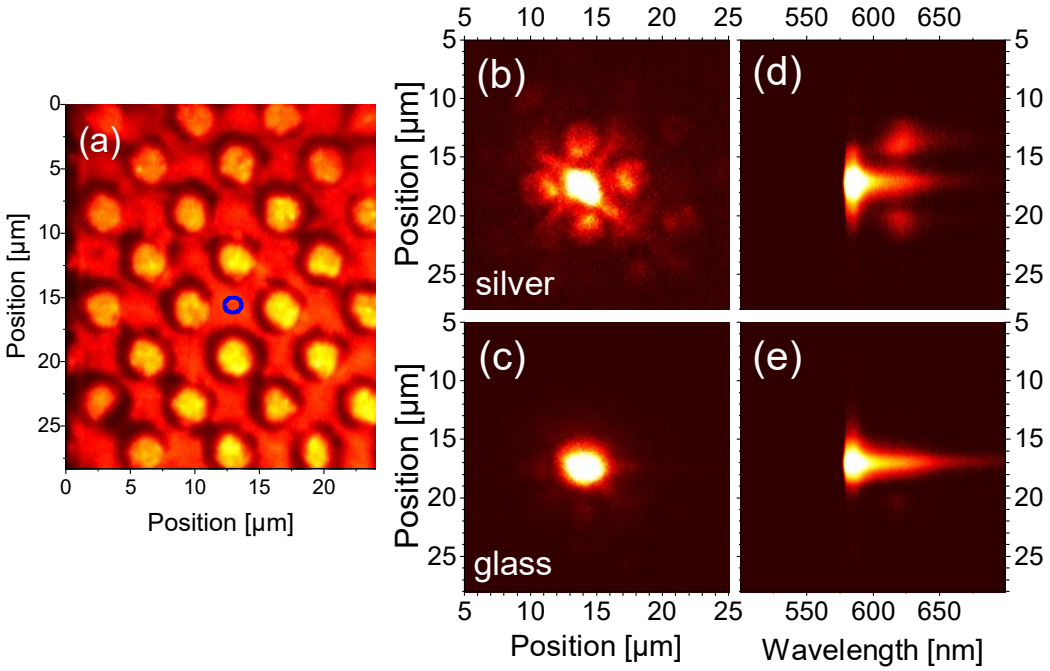

Figure 5. a) Luminescence image of an array where the dyes are spatially laterally separated excited on the whole image surface. The red circle corresponds to the position of the localized excitation spot used in the other panels. Direct images of luminescence under localized excitation for a dye array on b) silver and c) glass. Spatially (vertical axis) and spectrally (horizontal axis) resolved luminescence of the dye arrays on d) silver and e) glass. In panels b-e, the colour scale is chosen to have the same level of saturation. In a, b and c a linear color scale is used. In d and e a log scale has been chosen to highlight the acceptor emission.

The excitation is then focalised on a donor (TDBC) region, marked by the red open circle on Figure 5a. The luminescence images under localized excitation are shown in **Figure 5b** (dye array deposited on silver) and **Figure 5c** (dye array deposited on glass). In the presence of the metal film, we can clearly observe light emission from the disks which are located on the side of the excitation spot. On the contrary, when dyes are deposited on a glass substrate, the luminescence remains confined around the excitation spot. To show that such a spatially extended luminescence comes from the emission of the acceptor (i.e. the Cy3-Et dye) and not from donor's emission scattering, a spectral analysis is performed. A vertical stripe is selected in the direct images of Figure 5b and 5c and spectrally resolved. The resulting spectral images are shown on **Figure 5d** and **5e**. An emission at the acceptor energy spatially separated from the donor emission can be clearly seen on silver, showing the energy transfer on a scale of several microns. On the glass substrate only the donor emission can be observed.

To confirm the energy transfer, measurements with a larger excitation spot have been performed. For this purpose, a 532 nm laser diode was focused on a 50 µm diameter spot on the top side of the sample, illuminating around 50 patterns. The excitation energy is non-resonant with the dye absorptions and both materials are excited. The experimental emission is presented in **Figure 6a**. The black crosses correspond to the three polaritonic lines recorded in reflectometry on the same area of the sample (Figure 3a).

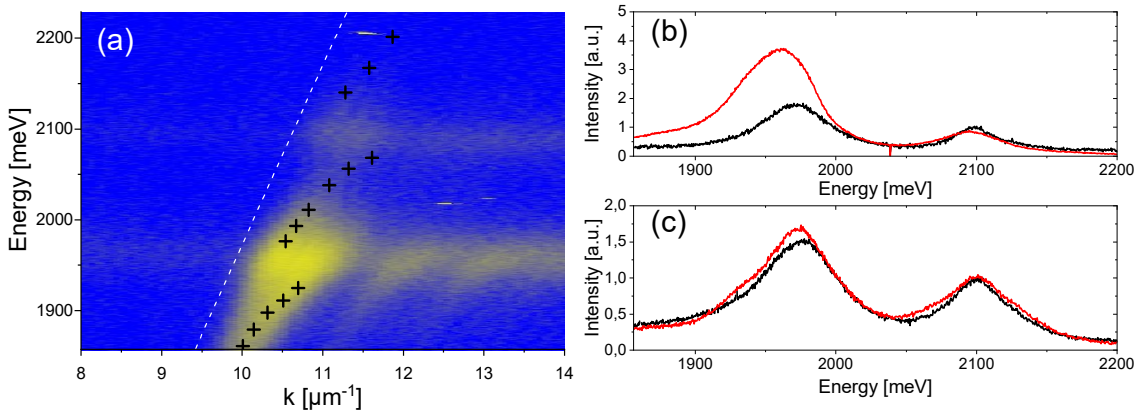

Figure 6. a) Emission dispersion of the polaritonic metasurface. The black crosses correspond to the experimental reflectometry dispersion lines of Fig. 3a. The dashed white line indicates the light cone. Emission spectra of dye arrays on silver (b) and glass substrates (c). The red lines correspond to the coherent states (N.A. >1), the black lines to the incoherent states (N.A. <1).

The emission in strong coupling can be separated in two contributions. [6] The first one is the coherent polaritonic emission, at the polariton wavevector/energy. This contribution is located under the light cone represented by a white dashed line on the Figure 6a. The contribution to this emission is mainly concentrated in the lower polariton (LP). Diffracted orders of the LP emission can also be seen on this figure, presenting the typical curvature of the anticrossing with the horizontal excitonic line, and the same wavevector shift of 1 μm^{-1} than in the reflectometry experiment. The second contribution is the dispersionless incoherent emission, which lies at the same energy as the bare excitonic states. This contribution appears as two weak horizontal lines at 1970 and 2100 meV (bare Cy3-Et and TDBC energies) in the dispersion images reported on Figure 6a. We have integrated the luminescence of the coherent and incoherent states separately, between N.A. = 1 and N.A. = 1.49 for the coherent contribution and below N.A. = 1 for the incoherent states. [8] The resulting spectra, recorded on the region were the dyes are spatially separated on silver, are shown in **Figure 6b**. For each spectrum, two peaks are present around 1970 and 2100 meV which can be attributed to Cy3-Et and TDBC, respectively. We define the ratio between the maximum emission of acceptor and donor as: $r = \frac{I_{max,Cy3-E}}{I_{max,TDBC}}$. For the coherent states this ratio is r_{coh} = 4.4, while for the incoherent states, taken as reference, r_{incoh} = 1.9. An enhancement of the acceptor emission of a factor 2 is thus measured for the coherent states, i.e. the hybrid states, confirming the energy transfer between the donor and the acceptor array. It should be noted that measurement on glass could also have been taken as a reference. Indeed, luminescence spectra recorded for the same dye pattern deposited on glass are shown on **Figure 6c**. The ratio of emission from the two dyes r ~ 1.7 is the same for numerical apertures smaller and larger than 1, and is of the same order of magnitude as the ratio measured for incoherent states on silver. The advantage of comparing coherent and incoherent contributions on a silver substrate instead of on glass is that it avoids any inhomogeneity contribution of the sample, as the data are taken on the same region.

5. Conclusion

In conclusion, a periodic structure formed by two spatially separated interlocking arrays of dyes was fabricated on a silver film. The hybridization of the two materials forming the arrays was shown by reflectometry measurements, compared with FDTD calculations and a coupled oscillator model. The intermediate polariton branch shows a quasi-equal mixture of the two

materials and the plasmon (30 % for the excitons and 40 % for the plasmon), which is a requirement for efficient strong coupling energy transfer. Luminescence experiments demonstrate energy transfer between the donor and acceptor lattices even though they are spatially separated by micrometric distances. The fabrication of such polaritonic metasurfaces can allow a control of the mixing and thus of the energy levels and polarizability with various parameters offered by the geometry. The transfer from one material to the other could find applications in the excitation of organic emitter with an efficient transfer and an easy access to the in-plane separated structures. Multimaterial strongly coupled metasurfaces can also be extended to the vibrational strong coupling where the control of the energy states could find applications in strong coupling chemistry.

Acknowledgements

The authors acknowledge financial support from French Agence Nationale de la Recherche on AAPG project 18-CE30-0014 PlasHybrid

The authors declare no conflict of interest

References

[1] E. Orgiu, J. George, J. A. Hutchison, E. Devaux, J. F. Dayen, B. Doudin, F. Stellacci, C. Genet, J. Schachenmayer, C. Genes, G. Pupillo, P. Samorì, T. W. Ebbesen, *Nat. Mater.* **2015**,*14*, 1123.

[2] J. Flick, N. Rivera, P. Narang, *Nanophotonics* **2018**, *7*, 1479.

[3] A. Thomas, E. Devaux, K. Nagarajan, G. Rogez, M. Seidel, F. Richard, C. Genet, M. Drillon, T.W. Ebbesen, *Nano Lett.* **2021**, *21*, 4365.

[4] C. Weisbuch, M. Nishioka, A. Ishikawa, Y. Arakawa, *Phys. Rev. Lett.* **1992**, *69*, 3314.

[5] J. Bellessa, C. Bonnand, J. C. Plenet, J. Mugnier, *Phys. Rev. Lett.* **2004**, *93*, 036404.

[6] V. M. Agranovich, M. Litinskaia, D. G. Lidzey, *Phys. Rev. B* **2003**, *67*, 085311.

[7] V. M. Agranovich, Y. N. Gartstein, *Phys. Rev. B* **2007**, *75*, 075302.

[8] S. Aberra Guebrou, C. Symonds, E. Homeyer, J. C. Plenet, Yu. N. Gartstein, V. M. Agranovich, J. Bellessa, *PRL* **2012**, *108*, 066401.

[9] L. Shi, T. K. Hakala, H. T. Rekola, J.-P. Martikainen, R. J. Moerland, P. Törmä, *PRL* **2014**, *112*, 153002.

[10] J. Feist, F.J. Garcia-Vidal, *Phys. Rev. Lett.* **2015**, *114*, 196402.

[11] K. Nagarajan, J. George, A. Thomas, E. Devaux, T. Chervy, S. Azzini, K. Joseph, A. Jouaiti, M. W. Hosseini, A. Kumar, C. Genet, N. Bartolo, C. Ciuti, T.W. Ebbesen, *ACS. Nano*. **2020**, *14*, 10219.

[12] A. Thomas, J. George, A. Shalabney, M. Dryzhakov, S.J. Varma, J. Moran, T. Chervy, X. Zhong, E. Devaux, C. Genet, J.A. Hutchison, T.W. Ebbesen, *Angew. Chem. Int. Ed.* **2016**, *55*, 11462.

[13] R.F. Ribeiro, L.A. Martínez-Martínez, M. Du, J. Campos-Gonzalez-Angulo, J. Yuen Zhou, *Chem.Sci.* **2018**, *9*, 6325.

[14] F. J. Garcia-Vidal, C. Ciuti, T. W. Ebbesen, *Science* **2021**, *373*, 178.

[15] N. Meinzer, W. L. Barnes, and I. R. Hooper, Nat. Photonics 8, 889 (2014)

[16] K. Chevrier, J. M. Benoit, C. Symonds, S. K. Saikin, J. Yuen-Zhou, J. Bellessa, *Phys. Rev. Lett.* **2019**, *122*, 173902.

[17] D. G. Lidzey, D. D. C. Bradley, A. Armitage, S. Walker, M. S. Skolnick, *Science* **2000**, *288*, 1620.

[18] J. Wenus, R. Parashkov, S. Ceccarelli, A. Brehier, J.-S. Lauret, M. S. Skolnick, E. Deleporte, D. G. Lidzey, *Phys. Rev. B* **2006**, *74*, 235212.

[19] D.M. Coles1, N. Somaschi, P. Michetti, C. Clark, P.G. Lagoudakis, P.G. Savvidis, D.G. Lidzey, *Nature Materials* **2014**, *13*, 712.

[20] K. Georgiou, P. Michetti, L. Gai, M. Cavazzini, Z. Shen, D. G. Lidzey, *ACS Photonics* **2018**, *5*, 258-266.

[21] F.J. Garcia-Vidal, J. Feist, *Science* **2017**, *357*, 1357.

[22] X. Zhong, T. Chervy, S. Wang, J. George, A. Thomas, J. A. Hutchison, E. Devaux, C. Genet, T. W. Ebbesen. *Angew. Chem. Int. Ed.* **2016**, *55*, 6202.

[23] X. Zhong, T. Chervy, L. Zhang, A. Thomas, J. George, C. Genet, J.A. Hutchison, T.W. Ebbesen, *Angew. Chem. Int. Ed.* **2017**, *56*, 9034.

[24] K. Georgiou, R. Jayaprakash, A. Othonos, D. G. Lidzey, *Angew. Chem. Int. Ed.* **2021**, *60*, 16661–16667.

[25] G. G. Paschos, N. Somaschi, S. I. Tsintzos, D. Coles, J. L. Bricks, Z. Hatzopoulos, D. G. Lidzey, P. G. Lagoudakis, P. G. Savvidis, *Sci. Rep.* **2017**, *7*, 11377.

[26] R. Jayaprakash, K. Georgiou, H. Coulthard, A. Askitopoulos, S. K. Rajendran, D. M. Coles, A. J. Musser, J. Clark, I. D. W. Samuel, G. A. Turnbull, P. G. Lagoudakis, David G. Lidzey, *Light: Science & Applications* **2019**, *8*, 81.

[27] E.E. Jelley. *Nature* **1936**, *138*, 1009.

[28] D. G. Lidzey, D. D. C. Bradley, T. Virgili, A. Armitage, and M. S. Skolnick *Phys. Rev. Lett.* **1999**, *82*, 3316.

[29] D. Li, C. Symonds, F. Bessueille, J. C. Plenet, A. Errachid, G. Wu, J. Shen, J. Bellessa. *J. Opt. A: Pure Appl. Opt*. **2009**, *11*, 065601.

[30] G. Decher *Science* **1997**, *277*, 1232.

[31] E. Guzman, R. G. Rubio, F. Ortega, *Advances in Colloid and Interface Science* **2020**, 102197.

*Antoine Bard, Sylvain Minot, Clémentine Symonds, Jean-Michel Benoit, Alban Gassenq, François Bessueille, Bruno Andrioletti, Camilo Perez, Kévin Chevrier, Yannick De Wilde, Valentina Krachmalnicoff, and Joel Bellessa**

Extended hybridization and energy transfer in multimaterial polaritonic metasurfaces

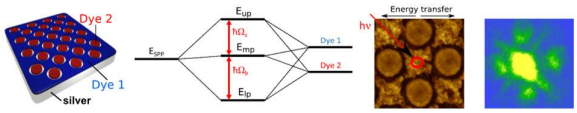

A Polaritonic metasurface is presented herein. It is composed of interlocked arrays of two organic materials on a silver surface. Both materials excitations are strongly coupled through the plasmon despite their spatial separation. The hybridization between both dyes leads to energy transfer over mircometric distances.